$(NHC^{Me})SiCl_4$: A Versatile Carbene Transfer Reagent – Synthesis From Silicochloroform

Supporting Information

Tobias Böttcher, Bassem S. Bassil, Lyuben Zhechkov, Thomas Heine and Gerd-Volker Röschenthaler*

School of Engineering and Science, Jacobs University Bremen, Campus Ring 1, D-28759 Bremen, Germany

Contents

1. Experimental Part 2
2. X-Ray Crystallography 6
3. NMR Spectra 12
4. Computational Results 18
5. Thermogravimetric Analysis 30
6. References 33

1. Experimental Part

All reactions were carried out under an atmosphere of dry nitrogen or argon with common Schlenk techniques in flame-dried glassware, as long as not stated otherwise. Acetonitrile and dichloromethane were distilled from CaH_2 under argon and were stored under 3 Å molecular sieves. Tetrahydrofuran, methyl *tert*-butyl ether and diethyl ether were distilled from sodium wire under argon and were stored under sodium wire. The deuterated solvents acetonitrile-d_3 and chloroform-d_1 were purchased from Eurisotop and were stored under 3 Å molecular sieves. ^{1}H, ^{13}C, ^{19}F, ^{31}P and ^{29}Si NMR spectra were recorded on a JEOL ECX 400 MHz spectrometer at room temperature using 5 mm tubes. The solvent signals were used as references and the chemical shifts converted to the TMS scale. For ^{29}Si, $Si(CH_3)_4$ was used as internal standard (δ Si = 0.00). Operating frequency: ^{1}H 400.53 MHz, ^{13}C 100.71 MHz, ^{19}F 376.88 MHz, ^{29}Si 79.57 MHz and ^{31}P 162.14 MHz. Mass spectrometric data was collected on a Bruker micrOTOF, fitted with an ESI source. Melting points were measured using a Jürgens Electrothermal Melting Point Apparatus. Thermogravimetric analysis was carried out on a TA Instruments SDT Q600 thermobalance. Elemental analysis was performed at Beller-Matthies laboratory in Sandersbeek 19, D-37085 Göttingen, Germany. 2-chloro-imidazolinium chloride (**1**) was prepared according to the literature.[13b] All other chemicals were purchased from available commercial sources.

$(NHC^{Me})SiCl_4$ (2). Method A: A solution of **1** (4.19 g, 24.79 mmol) in dichloromethane (30 ml) was placed into a Schlenk flask equipped with a septum. At -70 °C a solution of hexachlorodisilane (7.33 g, 27.27 mmol) in dichloromethane (15 ml) was slowly added through the septum using a syringe. After 1 h, the cooling bath was removed. The reaction mixture was stirred for another 3 h and was allowed to reach room temperature. All volatile components were removed under reduced pressure and the solid residue was washed with small amounts of cold acetonitrile and methyl *tert*-butyl ether. Drying *in vacuo* gave **2** (5.64 g, 85% based on **1**).

Method B: A suspension of **1** (7.26 g, 42.95 mmol) in tetrahydrofuran (120 ml) was placed in a 2-neck 500 ml flask equipped with a septum. Triethylamine (4.13 g, 40.81 mmol) was directly added through the septum using a syringe. After cooling to 0 °C, a solution of trichlorosilane (5.52 g, 40.75 mmol) in tetrahydrofuran (15 ml) was slowly added within 0.5 h through the septum using a syringe. After another 0.5 h, the ice bath was removed and the reaction mixture was stirred for 1 h and was allowed to reach room temperature. The suspension was filtered through a glass frit. All volatile components of the filtrate were removed under reduced pressure and the solid residue was washed with methyl *tert*-butyl ether followed by diethyl ether. Drying *in vacuo* gave **2** (9.61 g, 88% based on $HSiCl_3$). Colorless solid. M.p. 95 °C (dec). ^1H NMR (CD_3CN) $\delta = 3.39$ (s, 6H, $-CH_3$), 3.76 (s, 4H, $-CH_2-$). $^{13}C\{^1H\}$ NMR (CD_3CN) $\delta = 35.9$ (s, $-CH_3$), 52.4 (s, $-CH_2-$), 173.1 (s, carbene-C). ^{29}Si NMR (CD_3CN) $\delta = -103.9$ (s). Elemental analysis (%) calcd for $C_5H_{10}N_2SiCl_4$ (268.04): C, 22.40; H, 3.76; N, 10.45. Found: C, 22.53; H, 3.85; N, 10.40.

(NHC^{Me})PCl_3 (3a): A solution of **2** (1.32 g, 4.92 mmol) in tetrahydrofuran (40 ml) was placed into a 2-neck 100 ml Schlenk flask equipped with a septum. At 0 °C a solution of PCl_3 (0.74 g, 5.39 mmol) in tetrahydrofuran (15 ml) was added through the septum using a syringe. The mixture was stirred for additional 12 h and was allowed to reach room temperature. All volatile components were removed under reduced pressure. The residue was washed three times with diethyl ether. Drying *in vacuo* gave **3a** (1.14 g). Yield: 1.14 g (98% based on **2**). Colorless solid. ^1H NMR (CD_3CN) $\delta = 3.37$ (s, 6H, $-CH_3$), 3.79 (d, 4H, $-CH_2-$, $^4J_{HP} = 1$ Hz). $^{13}C\{^1H\}$ NMR (CD_3CN) $\delta = 36.0$ (d, $-CH_3$, $^3J_{CP} = 15$ Hz), 52.6 (s, $-CH_2-$), 172.9 (d, carbene-C, $^1J_{CP} = 109$ Hz). $^{31}P\{^1H\}$ NMR (CD_3CN) $\delta = 24.6$ (s). Elemental analysis (%) calcd for $C_5H_{10}N_2PCl_3$ (235.48): C, 25.50; H, 4.28; N, 11.90. Found: C, 25.72; H, 4.47; N, 11.99.

(NHC^{Me})PCl_2Ph (3b): 3b was prepared following the procedure for **3a**. Quantities used: **2** (2.02 g, 7.54 mmol), $PhPCl_2$ (1.48 g, 8.27 mmol). **3b** was obtained. Yield: 2.05 g (98% based on **2**). Colorless solid. ^1H NMR (CD_3CN) $\delta = 3.10$ (s, 6H, $-CH_3$), 3.78 (s, 4H, $-CH_2-$), 7.42 (m, 3H, *ortho*, *para* of –Ph), 8.17 (m, 2H, *meta* of -Ph). $^{13}C\{^1H\}$ NMR (CD_3CN) $\delta = 37.7$ (d, $-CH_3$, $^3J_{CP} = 11$ Hz), 52.3 (s, $-CH_2-$), 128.4 (m, *meta* of -Ph), 130.9 (s, *para* of -Ph), 136.4 (d, *ortho* of -Ph, $^2J_{CP} = 21$ Hz), 137.8 (d, *ipso* of –Ph, $^1J_{CP} = 41$ Hz), 174.86 (d, carbene-C, $^1J_{CP} = 78$ Hz). $^{31}P\{^1H\}$ NMR (CD_3CN) $\delta = -22.6$ (s). Elemental analysis (%) calcd for $C_{11}H_{15}N_2PCl_2$ (277.13): C, 47.67; H, 5.46; N, 10.11. Found: C, 47.51; H, 5.38; N, 9.96.

(NHC^{Me})PCl_2Me (3c): 3c was prepared following the procedure for **3a**. Quantities used: **2** (2.41 g, 8.99 mmol), $MePCl_2$ (1.17 g, 10.00 mmol). **3c** was obtained. Yield: 1.88 g (97% based on **2**). Colorless solid. ^1H NMR (CD_3CN) $\delta = 2.41$ (d, 3H, P-CH_3, $^2J_{PH} = 11$ Hz), 3.31 (s, 6H, $-CH_3$), 3.75 (s, 4H, $-CH_2-$). $^{13}C\{^1H\}$ NMR (CD_3CN) $\delta = 25.6$ (d, P-CH_3, $^1J_{PC} = 35$ Hz), 36.4 (d, N-CH_3, $^3J_{CP} = 14$ Hz), 52.3 (s, $-CH_2-$), 176.1 (d, carbene-C, $^1J_{CP} = 82$ Hz). $^{31}P\{^1H\}$

NMR (CD_3CN) δ = -22.1 (s). Elemental analysis (%) calcd for $C_6H_{13}N_2PCl_2$ (215.06): C, 33.51; H, 6.09; N, 13.03. Found: C, 33.49; H, 6.19; N, 13.01.

(NHC^{Me})PF_4H (4): A solution of **3a** (2.49 g, 10.57 mmol) in dichloromethane (60 ml) was placed in a 2-neck 250 ml flask equipped with a septum. At -40 °C triethylamine trihydrofluoride (2.60 g, 16.13 mmol) was added through the septum using a syringe, followed by dropwise addition of triethylamine (3.26 g, 32.22 mmol). During a period of 12 h, the reaction mixture was allowed to reach room temperature. All volatile components were removed under reduced pressure. The residue was suspended in ethanol and filtered through a glas frit, washed with small amounts of ethanol followed by diethyl ether. A solution of the crude product in acetonitrile was stored at -40 °C for 7 days to give crystals of **4**. Yield: 0.54 g (25% based on **3a**). Colorless solid. M.p.: 181 °C (dec). ^{1}H NMR (CD_3CN) δ = 3.20 (s, 6H, $-CH_3$), 3.71 (s, 4H, $-CH_2-$), 5.72 (d,quint, 1H, P-H, $^1J_{PH}$ = 938 Hz, $^2J_{HF}$ = 119 Hz). ^{19}F NMR (CD_3CN) δ = -49.1 (d,d, 4F, $^1J_{FP}$ = 839 Hz, $^2J_{FH}$ = 119 Hz). ^{13}C{^{1}H} NMR (CD_3CN) δ = 37.2 (m, $-CH_3$), 52.2 (d, $-CH_2-$, $^3J_{CP}$ = 11 Hz), 177.4 (d,quint, carbene-C, $^1J_{CP}$ = 292 Hz, $^2J_{CF}$ = 61 Hz). ^{31}P NMR (CD_3CN) δ = 141.9 (d,quint, $^1J_{PH}$ = 939 Hz, $^1J_{PF}$ = 839 Hz). HRMS (ESI, positive): m/z = 229.0477 (calcd for $[M+Na]^+$: 229.0488).

(NHC^{Me})$_2$$NiCl_2$ (5): A solution of **2** (3.51 g, 13.08 mmol) in tetrahydrofuran (80 ml) was placed into a 250 ml 2-neck flask equipped with a reflux condenser. Solid $Ni(PPh_3)_2Cl_2$ (2.67 g, 5.89 mmol) was added at once. The reaction mixture was refluxed for 12 h during which a orange/yellow solution was formed. The solution was cooled to room temperature. All volatile components were removed under reduced pressure. The residue was thoroughly washed with diethyl ether and then recrystallized from a hot acetonitrile solution. The solution was kept at -40 °C for 2 days to give **75**. Yield: 1.56 g (81% based on $Ni(PPh_3)_2Cl_2$). Orange-brown solid. M.p.: 212 °C (dec). Elemental analysis (%) calcd for $C_{10}H_{20}N_4NiCl_2$ (325.89): C, 36.85; H, 6.19; N, 17.19. Found: C, 36.76; H, 6.29; N, 17.03.

(NHC^{Me})$_2$$PdCl_2$ (6): A solution of **2** (2.54 g, 9.48 mmol) in tetrahydrofuran (80 ml) was placed in a 250 ml 2-neck flask. Finely grinded $PdCl_2$ (0.93 g, 5.24 mmol) was added as a solid at once. The reaction mixture was refluxed for 12 h during which a yellow solution was formed. The solution was cooled to room temperature. All volatile components were removed under reduced pressure. The residue was dissolved in dichloromethane and filtered through celite. The solvent was removed under reduced pressure and the residue was dissolved in acetonitrile and stored at -40 °C for 2 days to give **76**. Yield: 1.31 g (74 % based on **2**). Yellow solid. M.p.: 221 °C. ^{1}H NMR ($CDCl_3$) δ = 3.45 (s, 12H, -CH_3), 3.50 (s, 8H, -CH_2-). $^{13}C\{^{1}H\}$ NMR ($CDCl_3$) δ = 36.5 (s, -CH_3), 51.3 (s, -CH_2-), 198.3 (s, carbene-C). Elemental analysis (%) calcd for $C_{10}H_{20}N_4PdCl_2$ (373.62): C, 32.15; H, 5.40; N, 15.00. Found: C, 32.01; H, 5.47; N, 14.86.

2. X-Ray Crystallography

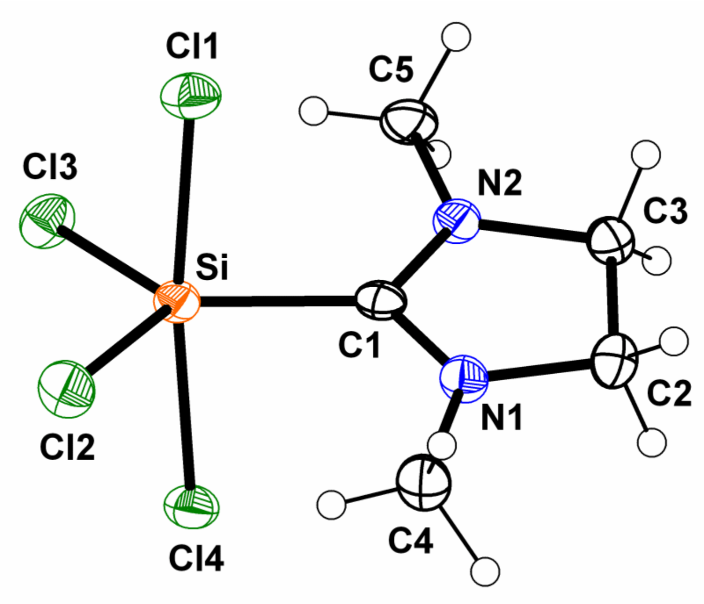

Figure S1. Atom labeling for the crystal structure of **2**.

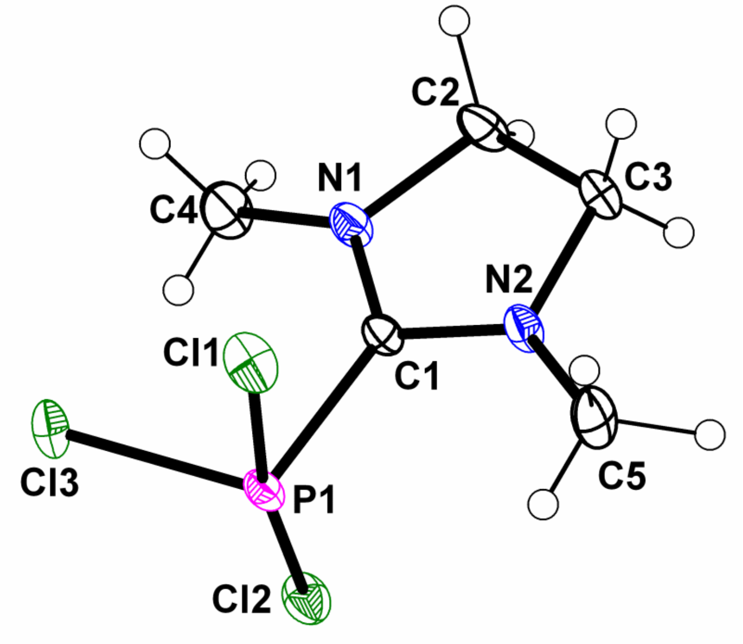

Figure S2. Atom labeling for the crystal structure of **3a**.

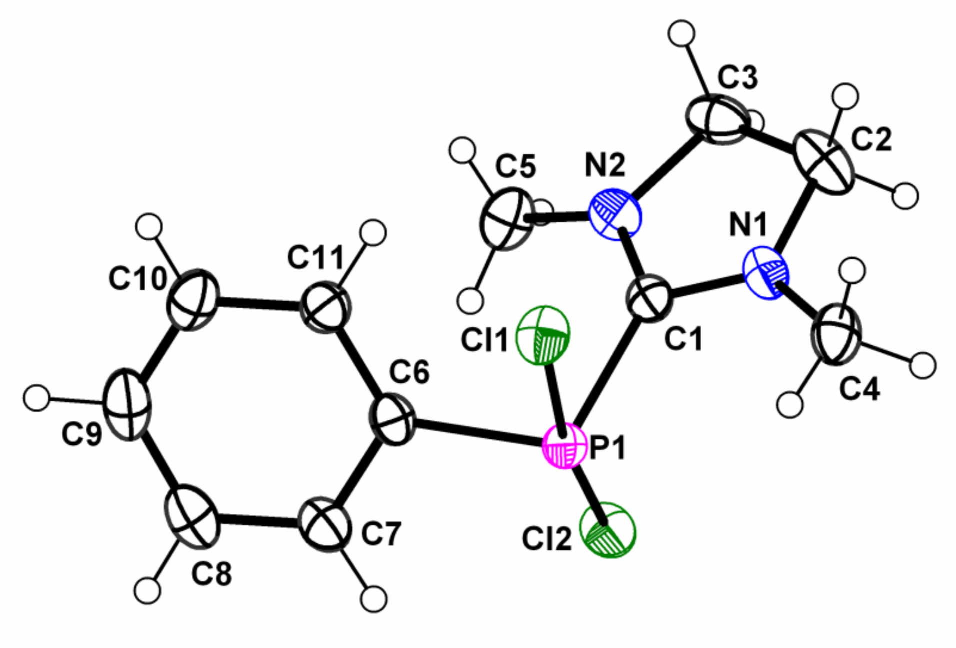

Figure S3. Atom labeling for the crystal structure of **3b**.

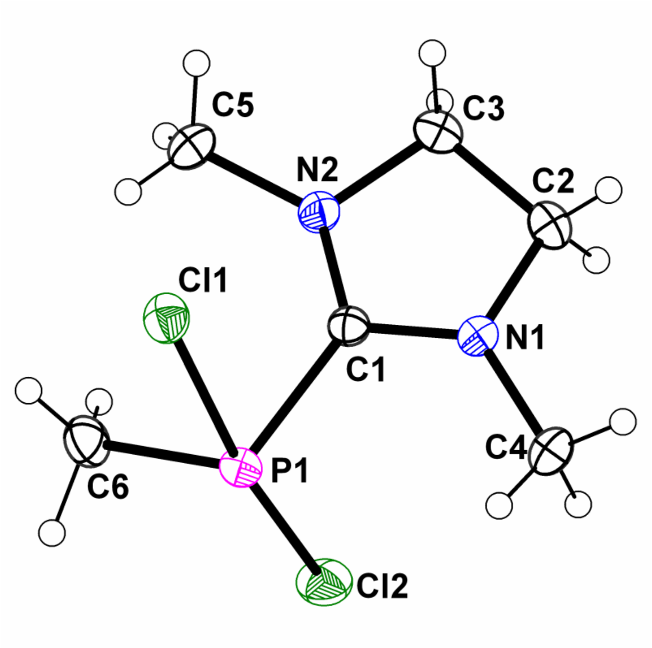

Figure S4. Atom labeling for the crystal structure of **3c**.

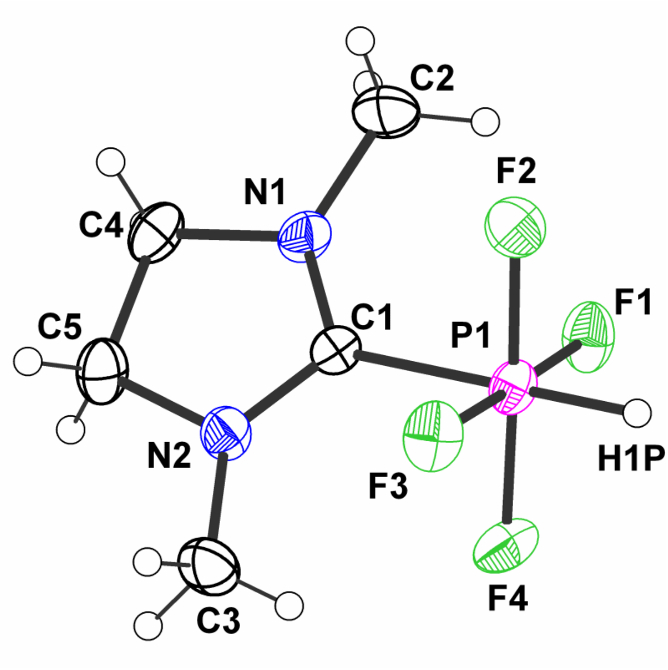

Figure S5. Atom labeling for the crystal structure of **4**.

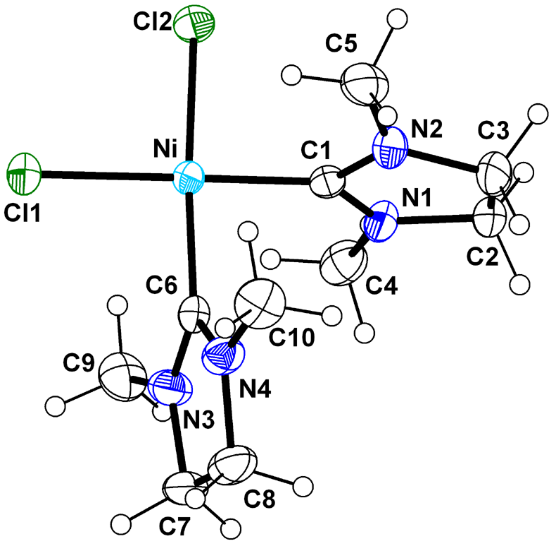

Figure S6. Atom labeling for the crystal structure of **5**.

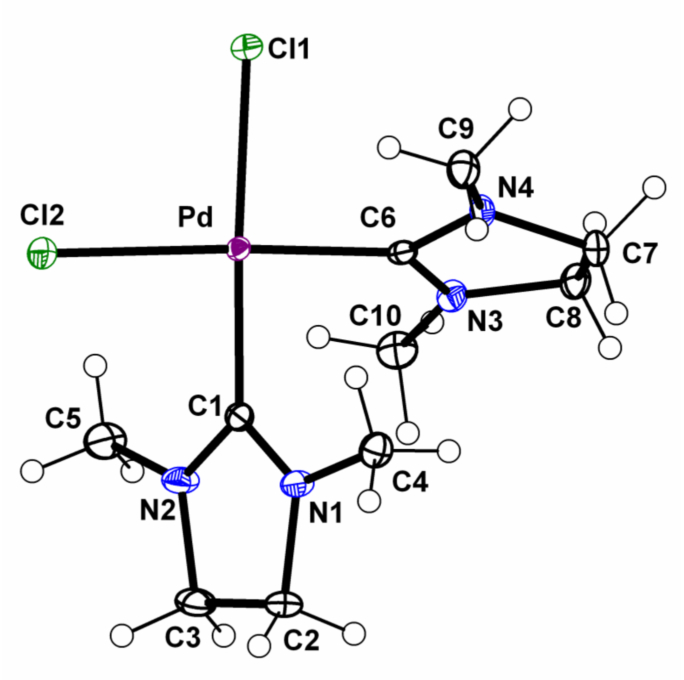

Figure S7. Atom labeling for the crystal structure of **6**.

Crystal structure determination

Crystal data for **3b, 3c, 4** and **5** was collected on a Siemens P4 diffractometer using graphite monochromated Mo Kα radiation (λ = 71.073 pm). Measurements were performed at -100°C by cooling with the low temperature nozzle Siemens LTII. The diffractometer was operated by the XSCAnS program. Single crystals of **2, 3a** and **6** were each mounted on a Hampton cryo-loop for indexing and intensity data collection at 100 K on a Bruker D8 APEX II CCD using Mo Kα radiation (λ = 71.073 pm). Lorentz and polarization corrections were applied, and an absorption correction was performed using the SADABS program.[1]

Direct methods were used for structure solution of all structures (SHELXS-97). Structural refinement was obtained from successive Fourier maps (SHELXL-97).[2] All heavy atoms (C, N, O, Si, P, Ni, Pd, F, Cl) were refined anisotropically whereas the hydrogen atoms were found either directly and refined isotropically for **2**, **3a**, **3b**, **3c**, **4, 6** or through calculated constrained positions for **5**.The crystallographic data for are summarized in Table S1.

Table S1. Crystal data for **2**, **3a**, **3b**, **3c**, **4**, **5** and **6**.

parameter	**2**	**3a**	**3b**	**3c**	**4**	**5**	**6**
Empirical formula	$C_5H_{10}Cl_4N_2Si$	$C_5H_{10}Cl_3N_2P$	$C_{11}H_{15}Cl_2N_2P$	$C_6H_{13}Cl_2N_2P$	$C_5H_{11}F_4N_2P$	$C_{10}H_{20}Cl_2N_4Ni$	$C_{10}H_{20}Cl_2N_4Pd$
Formular Weight	268.04	235.47	277.12	215.05	206.13	325.91	373.60
crystal system	Orthorhombic	Monoclinic	Monoclinic	Orthorhombic	Triclinic	Monoclinic	Monoclinic
space group	*Pbca*	$P2_1/c$	*C2/c*	*Pbca*	$P\bar{1}$	$P2_1/n$	$P2_1/n$
a (Å)	12.8424(6)	11.4381(10)	19.240(3)	7.768(2)	7.375(3)	8.0672(11)	8.9858(4)
b (Å)	12.6500(6)	7.7170(7)	11.531(3)	12.985(3)	7.560(2)	13.6398(12)	12.0174(6)
c (Å)	13.2356(6)	12.9790(11)	15.038(3)	19.423(4)	8.6846(15)	12.880(2)	13.4315(7)
α (deg)	90.00	90.00	90.00	90.00	74.688(16)	90.00	90.00
β (deg)	90.00	122.697(6)	128.66(3)	90.00	76.04(2)	100.756(13)	104.706(3)
γ (deg)	90.00	90.00	90.00	90.00	62.60(2)	90.00	90.00
volume (Å^3)	2150.21(17)	964.09(15)	2605.4(9)	1959.2(8)	410.5(2)	1392.4(3)	1402.90(12)
Z	8	4	8	8	2	4	4
D_{calcd} (g/cm^3)	1.656	1.622	1.413	1.458	1.667	1.555	1.769
abs coeff	1.163	1.057	0.596	0.769	0.351	1.762	1.688
F(000)	1088	480	1152	896	212	680	752
crystal size, mm^3	0.38 x 0.21 x 0.08	0.4 x 0.4 x 0.4	1.0 x 0.9 x 0.7	1.0 x 0.9 x 0.8	1.0 x 0.7 x 0.6	0.6 x 0.3 x 0.2	0.4 x 0.4 x 0.4
θ range for data collection (deg)	3.46 – 23.25	3.73 – 30.50	3.47 – 27.49	3.71 – 27.50	3.52 – 27.48	3.55 – 26.36	3.56 – 30.51
reflections collected	53047	53367	6638	5553	2344	6878	93989
independent reflections	1528	2934	2974	2243	1875	2837	4274
R(int)	0.1073	0.0518	0.0354	0.0296	0.0403	0.0664	0.0501
observed ($I > 2\sigma(I)$)	1247	2730	2680	2033	1767	2486	3890
goodness-of-fit on F^2	1.024	1.018	1.008	1.012	1.012	1.023	1.011
$R_1[I > 2\sigma(I)]^a$	0.0288	0.0309	0.0305	0.0316	0.0537	0.0310	0.0260
R_w (all data)^b	0.0819	0.0869	0.1014	0.0879	0.1532	0.0847	0.0773

$^aR_1 = \Sigma||F_o| - |F_c||/\Sigma|F_o|$. $^bR_w = \{\Sigma[w(F_o^2 - F_c^2)^2]/\Sigma[w(F_o^2)^2]\}^{1/2}$.

3. NMR Spectra

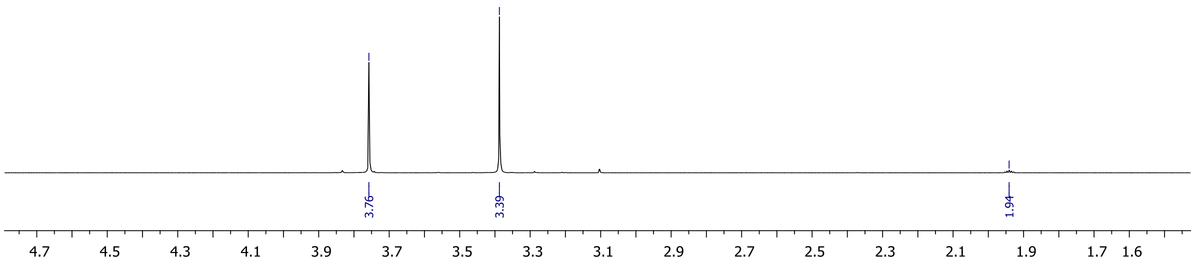

Figure S8. ^{1}H NMR of **2**.

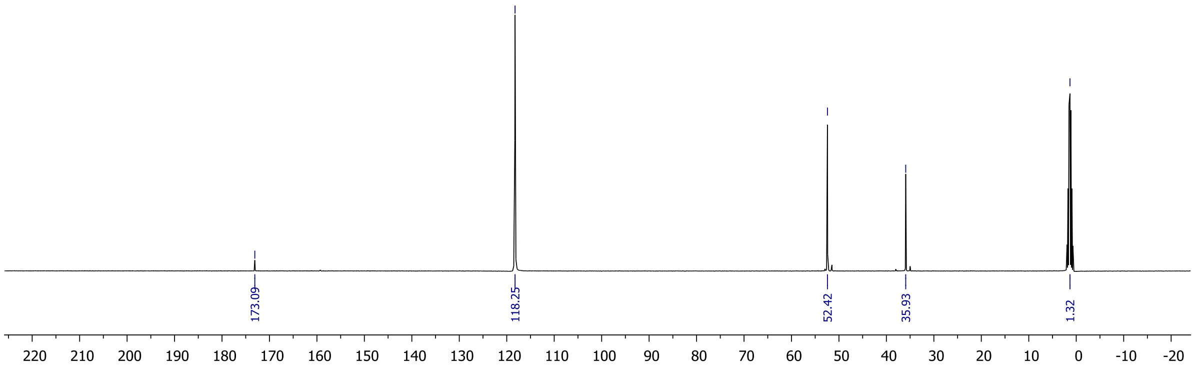

Figure S9. ^{13}C{^{1}H} NMR of **2**.

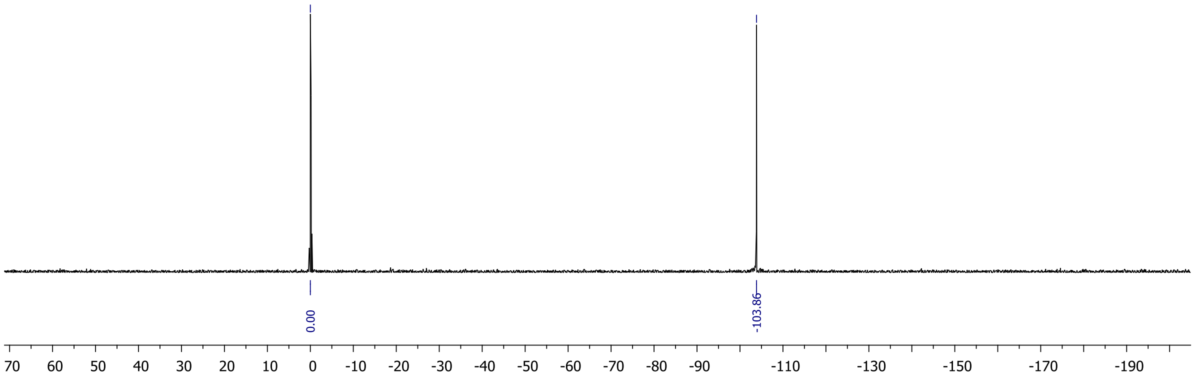

Figure S10. ^{29}Si NMR of **2**.

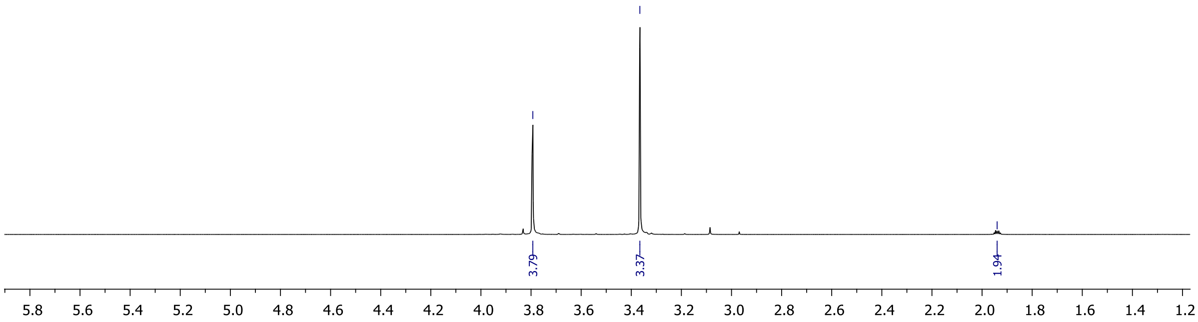

Figure S11. ^{1}H NMR of **3a**.

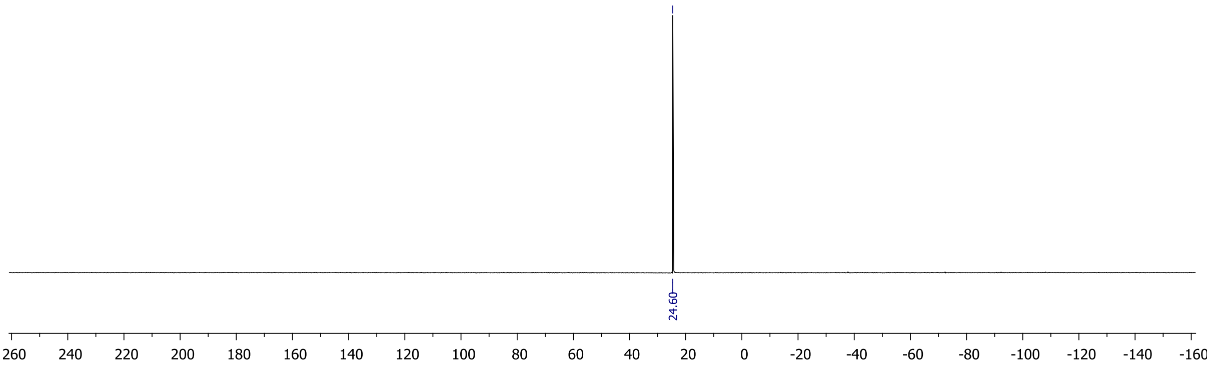

Figure S12. ^{31}P{^{1}H} NMR of **3a**.

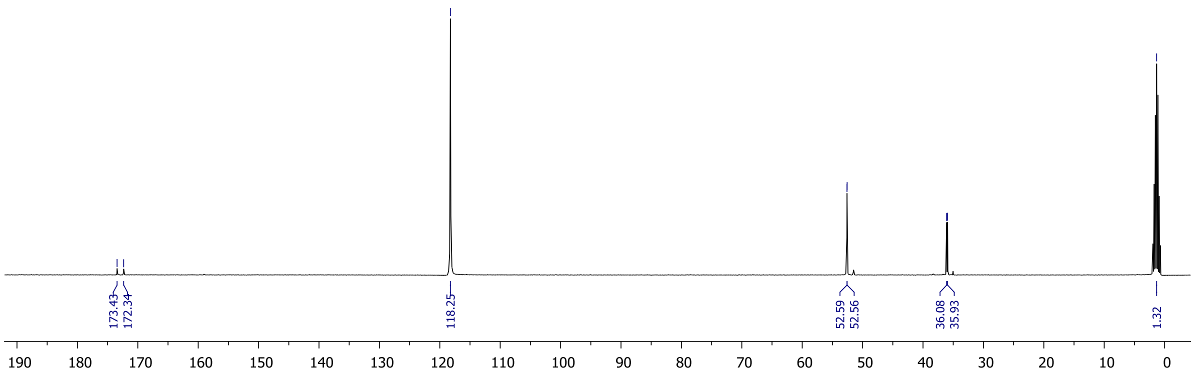

Figure S13. ^{13}C{^{1}H} NMR of **3a**.

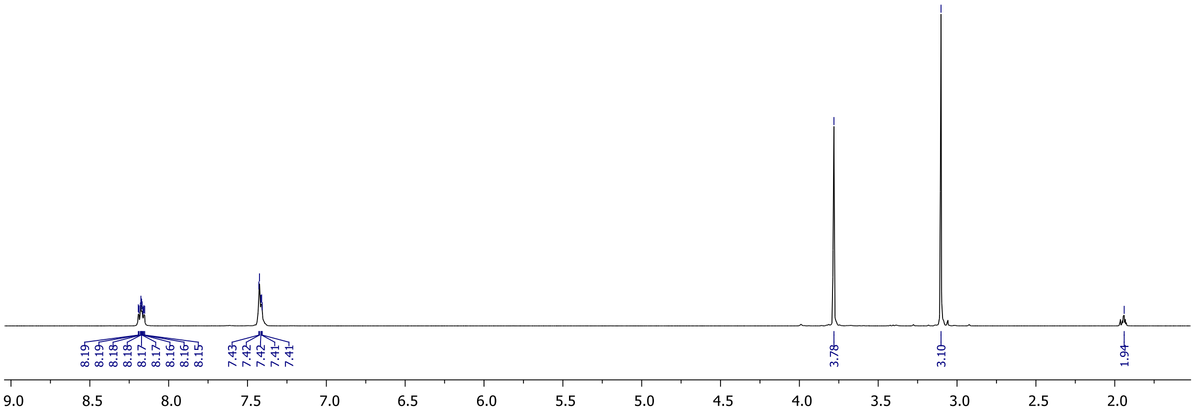

Figure S14. ^{1}H NMR of **3b**.

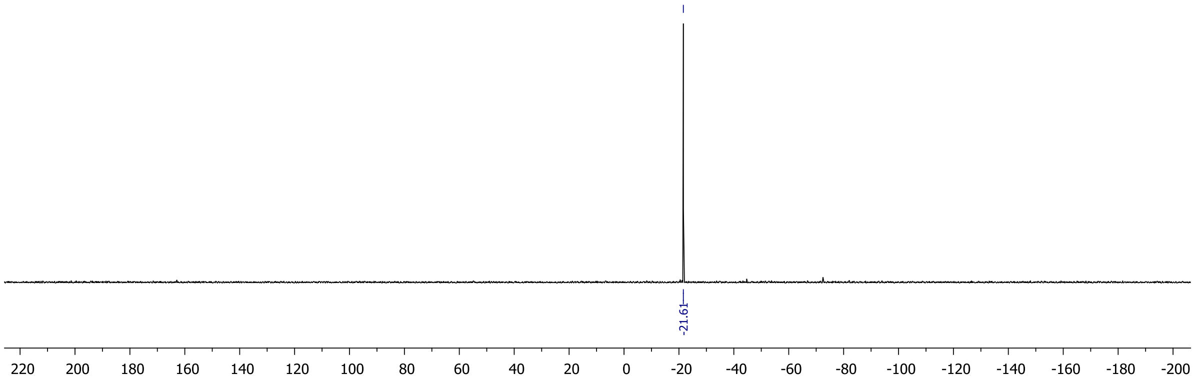

Figure S15. ^{31}P{^{1}H} of **3b**.

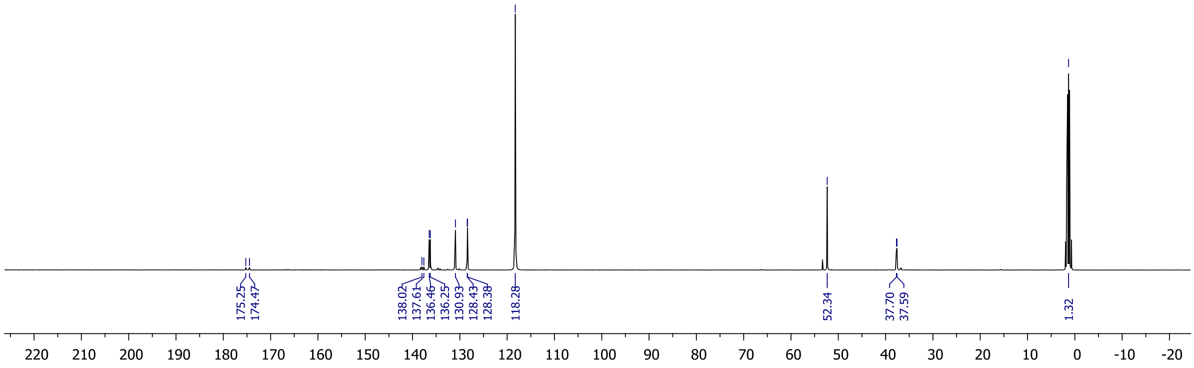

Figure S16. ^{13}C{^{1}H} NMR of **3b**.

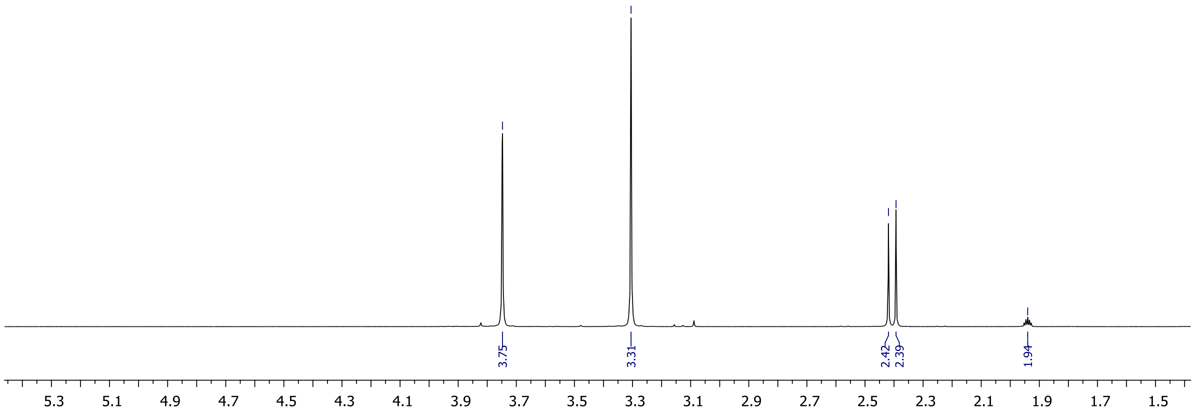

Figure S17. ^{1}H NMR of **3c**.

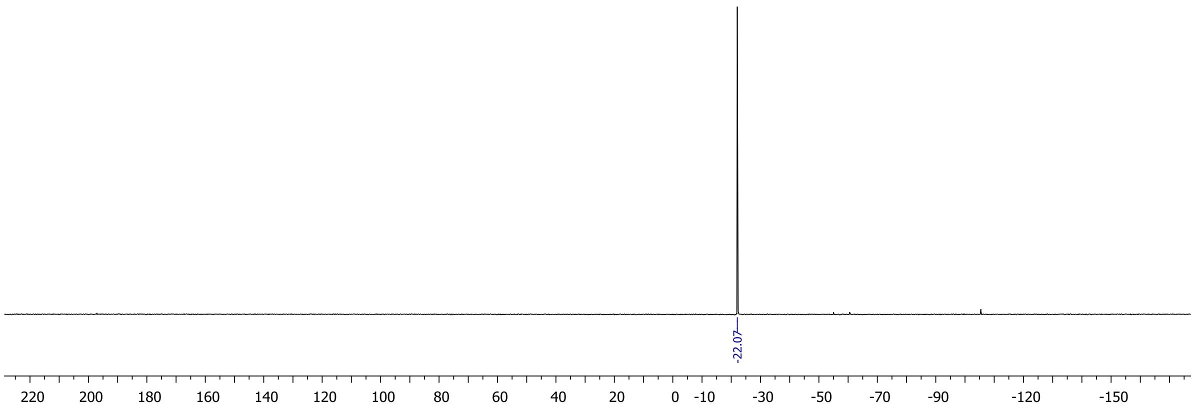

Figure S18. ^{31}P{^{1}H} NMR of **3c**.

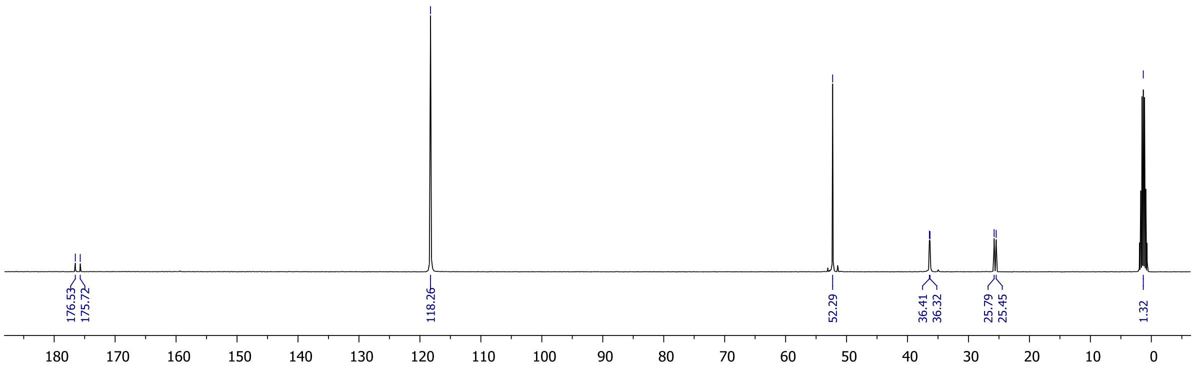

Figure S19. ^{13}C{^{1}H} NMR of **3c**.

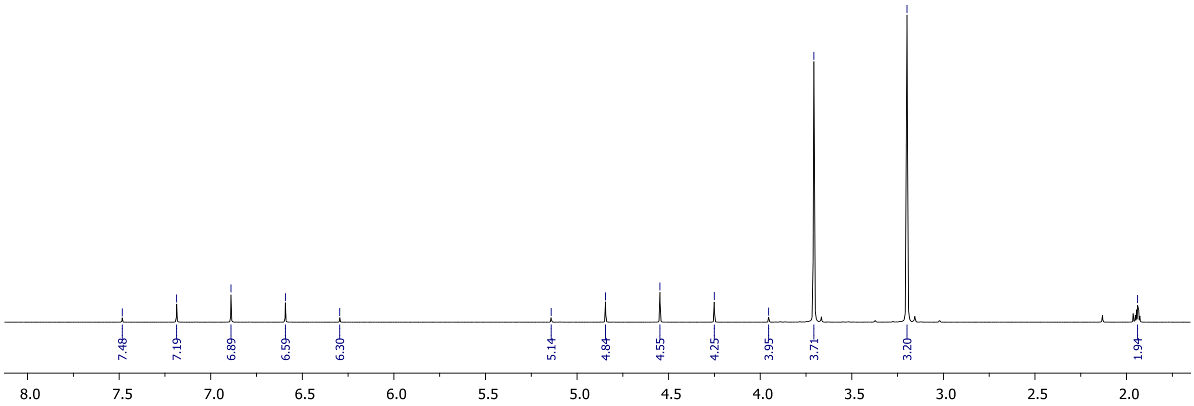

Figure S20. ^{1}H NMR of **4**.

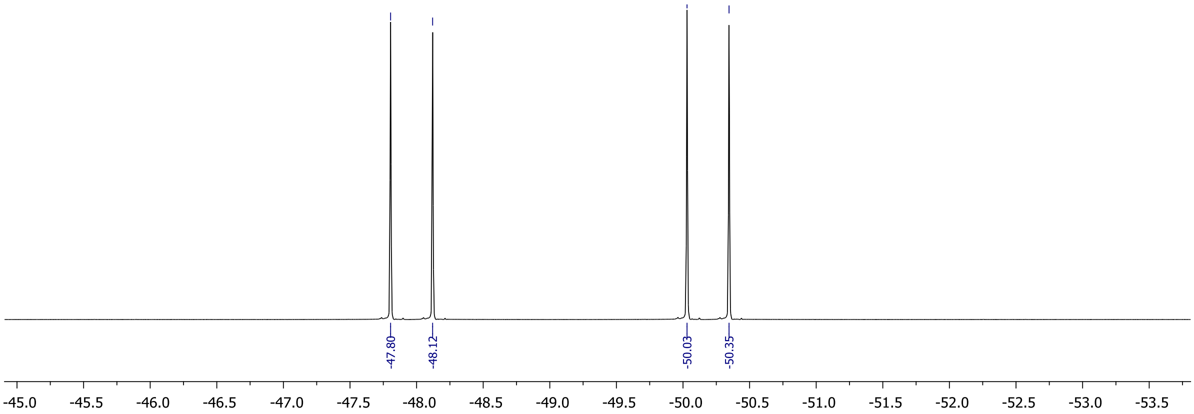

Figure S21. ^{19}F NMR of **4**.

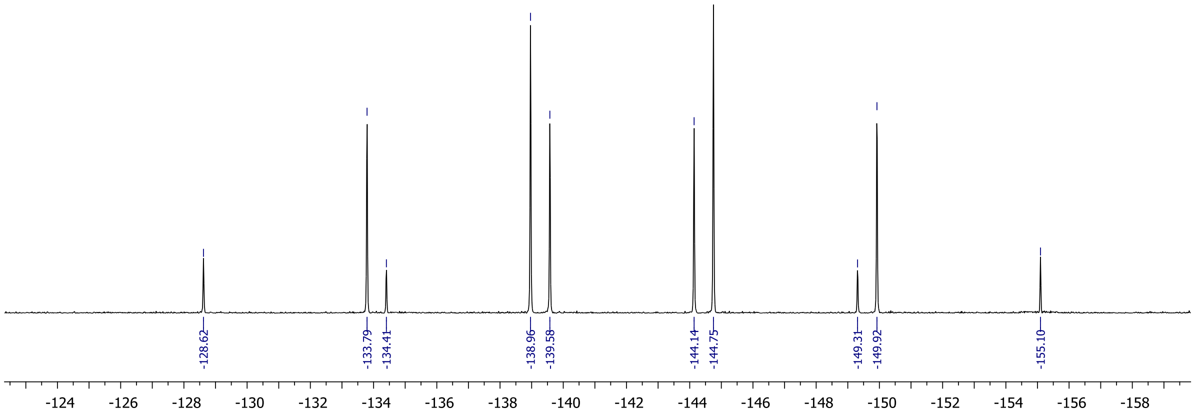

Figure S22. ^{31}P NMR of **4**.

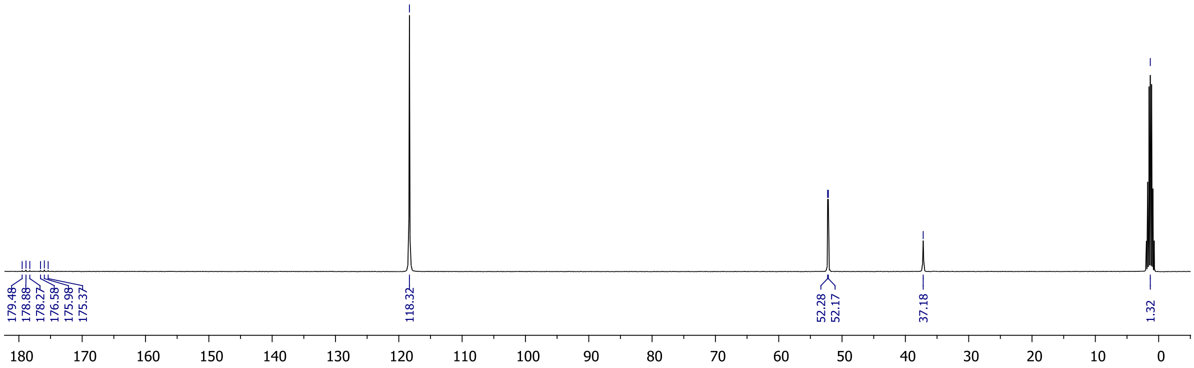

Figure S23. $^{13}C\{^1H\}$ NMR of **4**.

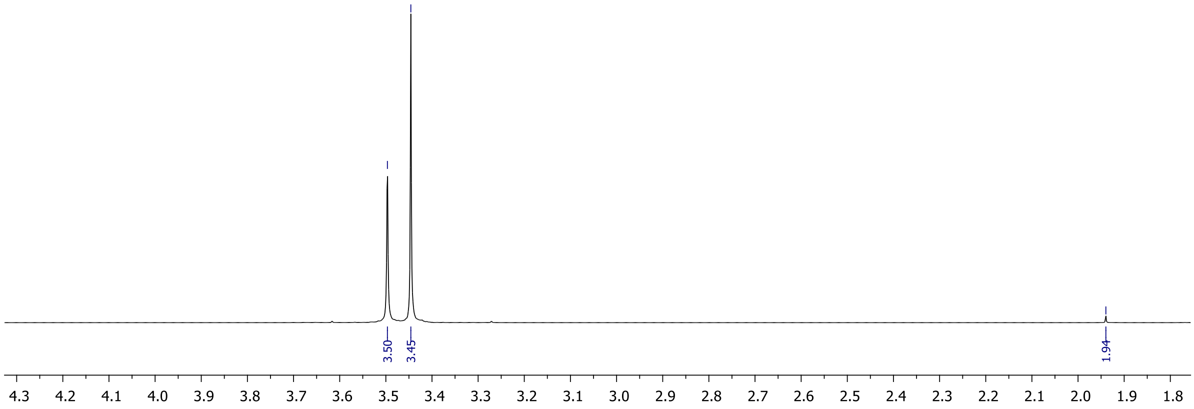

Figure S24. ^1H NMR of **6**.

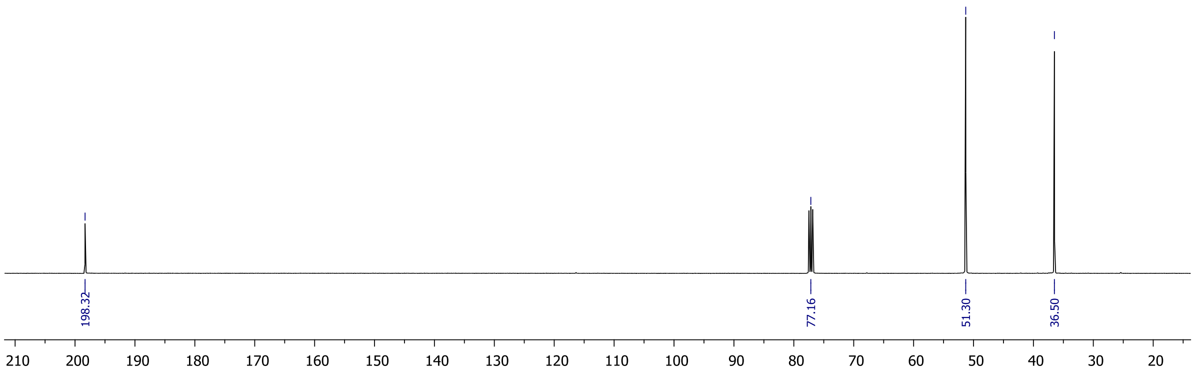

Figure S25. $^{13}C\{^1H\}$ NMR of **6**.

4. Computational Results

The computational results have been produced with full electron DFT[3] calculations using the adf2010.02 package.[4] The PBE[5] functional has been emplopoyed together with full electron TZ2P ZORA[6] basis sets for all atoms. Scalar relativistic correction has been applied for all calculations. For the analysis of the chemical bonding, we carried out fragment analyses to assess the C-Si and C-P bonds, and NBO[7] and AIM[8] analyses to obtain a general picture of the bonding in the molecules studied here. The coordinates of the optimized structures as well the charges, correlation diagrams and information for the contributions of the symmetrized fragment orbitals are listed below. The charge transfer through the C-Si bond has been evaluated as a change of the charge in the neutral fragments with respect to the charge of the same fragments in the complex. The total charge of the $SiCl_4$ fragment (-0.376 e^-) is calculated as a sum of the Si and Cl atomic charges in the complex. This leads to a conclusion that the direct electrostatic interaction (C-Si) is accompanied with transfer of electrons from the NHC to $SiCl_4$ fragment.

4.1. Data for $(NHC^{Me})SiCl_4$ (2).

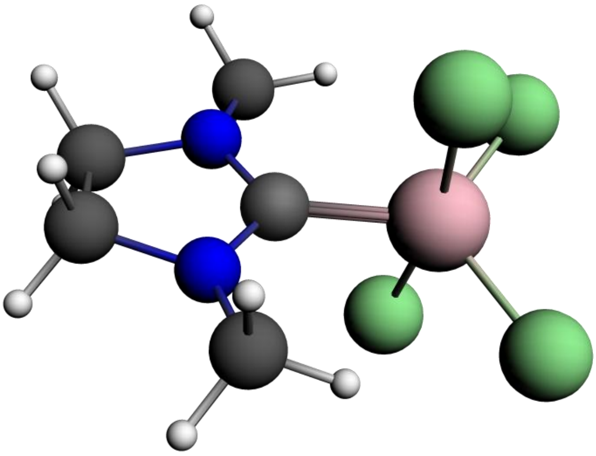

Figure S26. Structure of compound **2**.

Table S2. Coordinates of **2**.

atom	No	X	Y	Z
Si	1	0	0	0
Cl	2	-1.6407	1.4945	0.2329
Cl	3	-1.1929	-1.2999	-1.1351
Cl	4	1.1843	1.2857	-1.1601
Cl	5	1.6416	-1.4903	0.2411

C	6	0.0051	0.013	1.9572
C	7	-0.2531	-0.6891	4.153
C	8	0.2714	0.7468	4.1415
C	9	-1.06	-2.2214	2.3232
C	10	1.0716	2.2522	2.2863
H	11	-1.1395	-0.8247	4.7865
H	12	0.5205	-1.4148	4.4594
H	13	1.1597	0.892	4.7702
H	14	-0.5014	1.4766	4.4401
H	15	-1.3606	-2.2049	1.272
H	16	-1.9291	-2.4921	2.9372
H	17	-0.2664	-2.9741	2.4533
H	18	1.3867	2.215	1.2399
H	19	0.2727	3.0034	2.3894
H	20	1.931	2.5398	2.9062
N	21	-0.5892	-0.9085	2.7336
N	22	0.6029	0.9452	2.7182

Table S3. NBO Charges of (NHC^{Me})SiCl$_4$ (**2**).

Natural Population						
Atom	No	Charge	Core	Valence	Rydberg	Total
Si	1	1.10869	9.99866	2.76758	0.12507	12.89131
Cl	2	-0.42586	9.99972	7.4117	0.01444	17.42586
Cl	3	-0.31669	9.99954	7.29767	0.01947	17.31669
Cl	4	-0.31679	9.99954	7.29778	0.01947	17.31679
Cl	5	-0.42543	9.99972	7.41123	0.01448	17.42543
C	6	0.15653	1.99901	3.79198	0.05248	5.84347
C	7	-0.26194	1.99942	4.24873	0.01379	6.26194
C	8	-0.26193	1.99942	4.24871	0.0138	6.26193
C	9	-0.45347	1.99938	4.44126	0.01284	6.45347
C	10	-0.4538	1.99938	4.44158	0.01285	6.4538
H	11	0.22535	0	0.77215	0.0025	0.77465
H	12	0.21512	0	0.78057	0.00431	0.78488
H	13	0.22531	0	0.77219	0.0025	0.77469
H	14	0.21517	0	0.78052	0.00431	0.78483

H	15	0.24189	0	0.75538	0.00272	0.75811
H	16	0.21562	0	0.78247	0.00191	0.78438
H	17	0.21897	0	0.77768	0.00335	0.78103
H	18	0.24178	0	0.75551	0.0027	0.75822
H	19	0.21947	0	0.77717	0.00337	0.78053
H	20	0.2157	0	0.78241	0.00189	0.7843
N	21	-0.29175	1.99934	5.27095	0.02147	7.29175
N	22	-0.29194	1.99934	5.27112	0.02148	7.29194
Total		0	63.99246	71.63633	0.37121	136

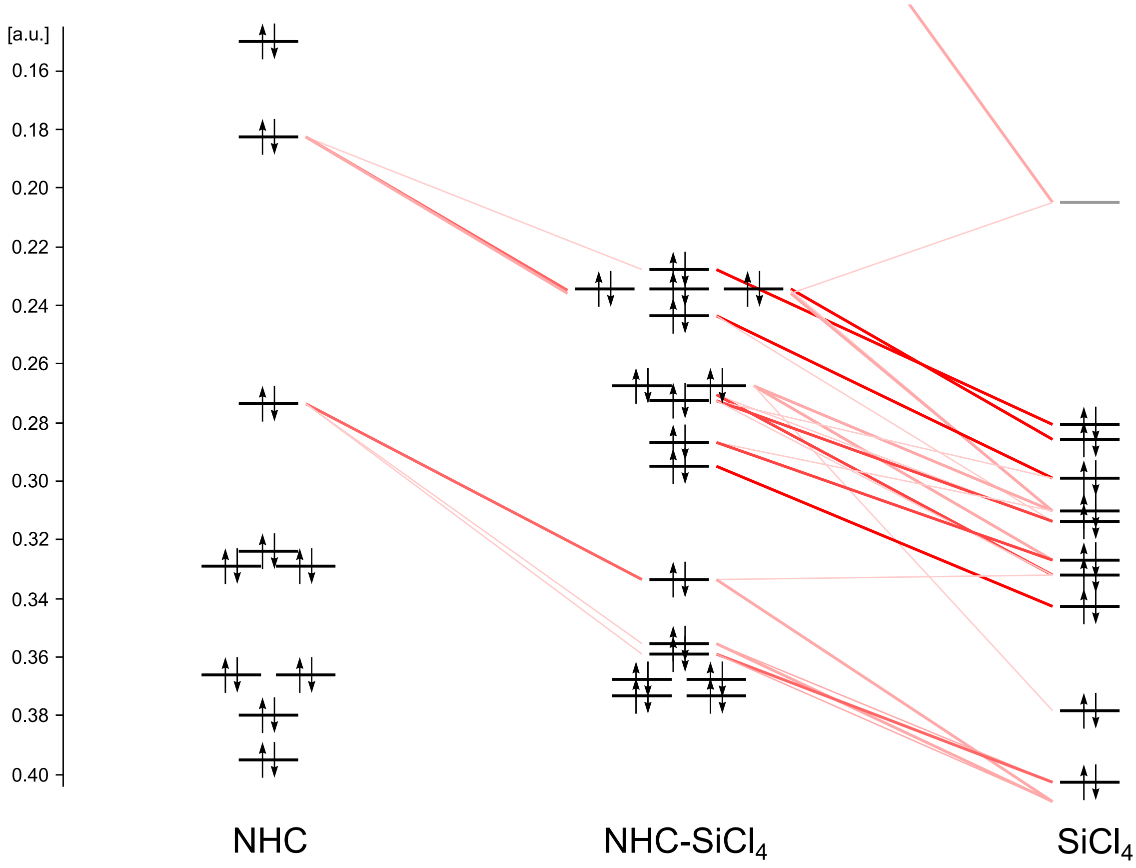

Figure S27. Correlation diagram of **2**. Left column: NHC-fragment molecular orbitals; Middle column: full complex molecular orbitals; Right column: SiCl$_4$ molecular orbitals. The thickness of the lines corresponds to the contribution of the fragment molecular orbitals to the complex molecular orbitals.

Table S4. Decomposition of the (NHC^{Me})SiCl$_4$ HOMO orbital into symmetrized fragment orbitals.

fragment/atom number	fragment	atom	contribution to HOMO	orbital type	Energy (eV)	occupation
1	SiCl4		86.52%	41 A	-7.633	2
3		Cl	13.89%	2 P:x	-8.581	1.67
2		Cl	13.45%	2 P:y	-8.581	1.67
5		Cl	13.28%	2 P:y	-8.581	1.67
4		Cl	11.94%	2 P:y	-8.581	1.67
3		Cl	11.85%	2 P:y	-8.581	1.67
2		Cl	10.87%	2 P:x	-8.581	1.67
5		Cl	10.68%	2 P:x	-8.581	1.67
2	NHC		10.06%	26 A	-4.971	2
17		N	28.70%	1 P:x	-7.089	1
16		N	28.64%	1 P:x	-7.089	1
17		N	7.30%	1 P:y	-7.089	1
16		N	7.29%	1 P:y	-7.089	1
1	SiCl4		2.94%	34 A	-9.330	2
5		Cl	13.72%	2 P:y	-8.581	1.67
2		Cl	13.60%	2 P:y	-8.581	1.67
4		Cl	12.49%	2 P:x	-8.581	1.67
3		Cl	12.42%	2 P:x	-8.581	1.67
5		Cl	11.24%	2 P:x	-8.581	1.67
2		Cl	11.17%	2 P:x	-8.581	1.67
3		Cl	10.45%	2 P:y	-8.581	1.67
4		Cl	10.36%	2 P:y	-8.581	1.67

Table S5 Energy Decomposition Analysis (EDA).

The following table summarizes the computational results of the EDA for compounds that are representative for ionic and donor-acceptor bonds. The data for the compounds investigated by us and Liu[9], and the data for NHC-AgCl are given at the bottom of the table for comparison. The table compares the oribital, electrostatic, Pauli, and total binding energies. As described in ref. [10], they can be used to identify the covalent and the electrostatic contribution to the bond. The table also contains a column with the values of the charge transfer between the fragments in the complex. These are calculated using Natural Population Analysis (NPA), as a difference between the total charge of the isolated fragment and the charge of the same fragment in the complex.

Molecule	Total binding energy	Pauli repulsion	Electrostatic interaction	Orbital interaction	NPA charge transfer
$[CH_3O]^{-}$-Na^{+}	-152.51	26.54	-156.49	-22.56	0.041
$[CH_3O]^{-}$-K^{+}	138.43	41.4	-149.34	-30.49	0.047
H_3B-NH_3	-47.40	110.67	-78.78	-79.27	0.397
$[H_3N$-$H]^{+}$	-210.85	0.0	-40.39	-169.92	0.53
$[H_2O$-$H]^{+}$	-170.4	0.0	-24.27	-146.17	0.4
NHC-$SiCl_4$	68.1	235.4	-169.96	-136.51	0.37
NHC-AgCl	-55.8	128.32	-143.96	-41.04	0.189
NHC-$SiCl_4$ [a]	-72.44	232.21	-143.10	-136.28	0.41

a) The compound has been investigated in article published by Liu[9] however the data published in this table has been recalculated with the methods and basis sets used for the other compounds in this table.

Data for (NHC^{Me})PCl$_3$ (3a).

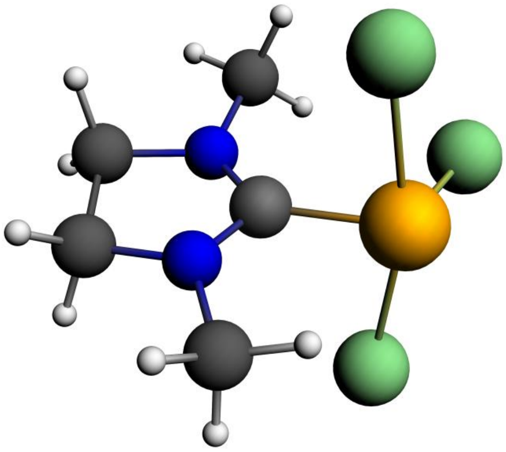

Figure S28. Structure of compound **3a**.

Table S6. Coordinates of **3a**.

Atom	No	X	Y	Z
H	1	-2.39498	1.929933	3.509708
H	2	-1.25666	1.886398	4.882209
H	3	-2.56098	0.650669	4.736133
H	4	-0.07607	-2.20159	2.409563
H	5	1.473246	-1.67916	3.144174
H	6	0.353201	-0.39548	4.847935
H	7	-1.05573	-1.43787	4.474526
H	8	1.676807	0.390874	0.264006
H	9	0.295491	-0.67021	-0.14547
H	10	1.752096	-1.34257	0.664349
N	11	0.519045	-0.23605	1.911702
N	12	-0.97489	0.396302	3.411318
C	13	-0.39164	0.689333	2.23963
C	14	0.46135	-1.35647	2.871229
C	15	-0.31454	-0.7519	4.045147
C	16	1.09071	-0.47243	0.588625
C	17	-1.8402	1.267861	4.183954
P	18	-0.98983	2.243838	1.355798
Cl	19	0.270266	2.545511	-0.27974
Cl	20	0.487777	3.322816	2.821258
Cl	21	-2.30643	0.657753	0.211914

Table S7. NBO charges of **3a**.

Atom	No	Charge	Core	Valence	Rydberg	Total
H	1	0.23515	0	0.76146	0.00339	0.76485
H	2	0.22836	0	0.76804	0.00359	0.77164
H	3	0.21995	0	0.77794	0.0021	0.78005
H	4	0.2174	0	0.7783	0.0043	0.7826
H	5	0.22595	0	0.77145	0.0026	0.77405
H	6	0.21646	0	0.77902	0.00452	0.78354
H	7	0.22534	0	0.772	0.00267	0.77466
H	8	0.23971	0	0.75766	0.00262	0.76029
H	9	0.23663	0	0.75973	0.00364	0.76337
H	10	0.21648	0	0.782	0.00153	0.78352
N	11	-0.29938	1.99929	5.2763	0.02379	7.29938
N	12	-0.29546	1.99931	5.27324	0.02291	7.29546
C	13	0.27248	1.9991	3.6857	0.04272	5.72752
C	14	-0.25646	1.99941	4.24405	0.013	6.25646
C	15	-0.25879	1.99941	4.24589	0.01348	6.25879
C	16	-0.45707	1.99937	4.44395	0.01375	6.45707
C	17	-0.45216	1.99937	4.43937	0.01342	6.45216
P	18	0.63865	9.9989	4.26438	0.09808	14.36135
Cl	19	-0.22561	9.99973	7.20362	0.02227	17.22561
Cl	20	-0.46055	9.9999	7.44907	0.01158	17.46055
Cl	21	-0.4671	9.99991	7.456	0.01119	17.4671
Total		0	53.9937	65.68916	0.31713	120

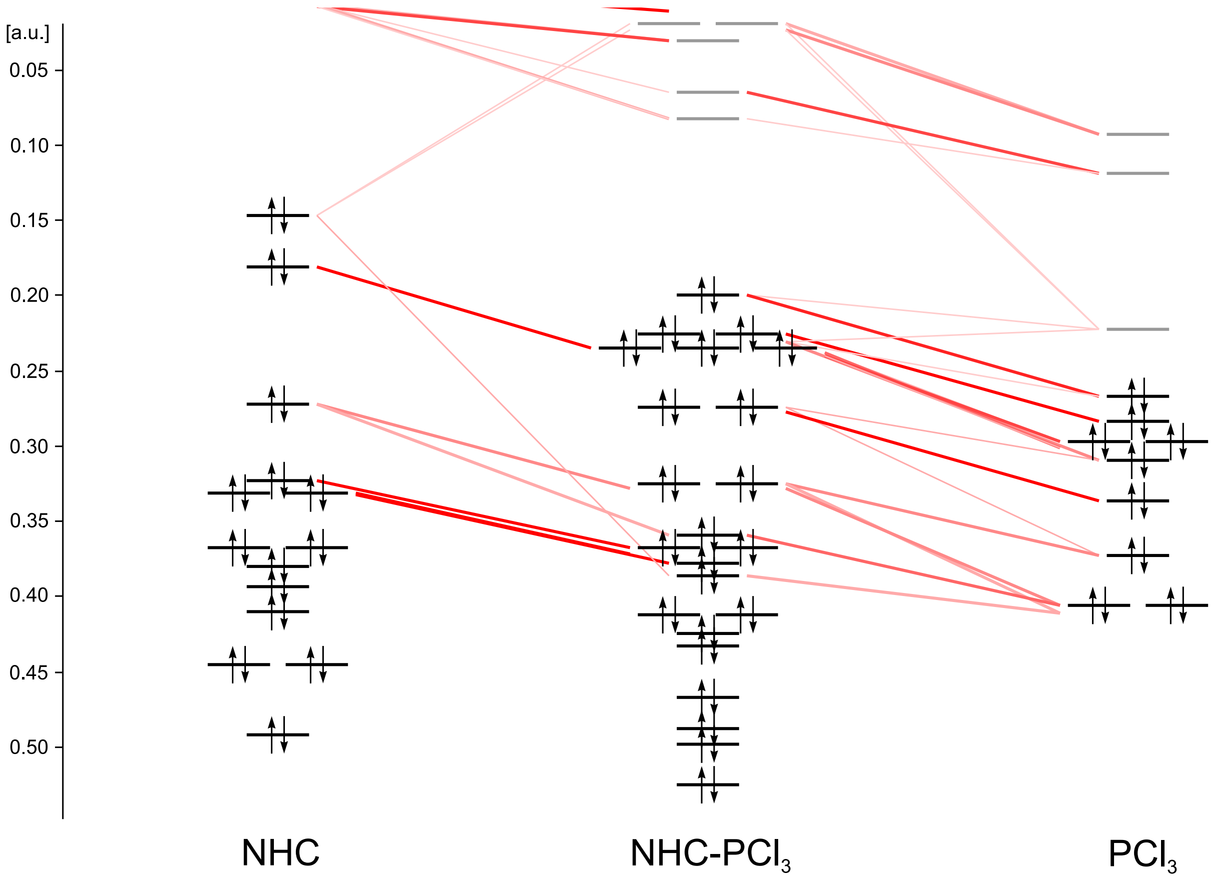

Figure S29. Correlation diagram of **3a**. Left column: NHC-fragment molecular orbitals; Middle column: full complex molecular orbitals; Right column: PCl_3 molecular orbitals. The thickness of the lines corresponds to the contribution of the fragment molecular orbitals to the complex molecular orbitals.

4.2. Data for $(NHC)_2NiCl_2$ (5).

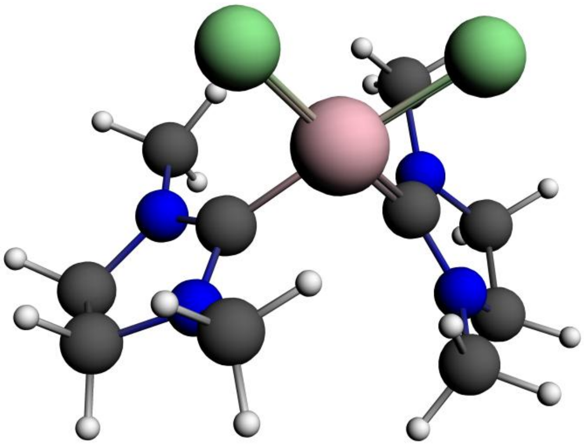

Figure S30. Complex **5**.

Table S8. Coordinates of **5**.

atom	No	X	Y	Z
Ni	1	-0.1881	0.0018	0
Cl	2	1.3002	-0.3921	-1.5888
Cl	3	1.3008	0.3933	1.589
C	4	-1.4256	0.168	1.3644
C	5	-3.0418	1.0244	2.8341
C	6	-2.585	-0.3516	3.3322
C	7	-2.0485	2.5546	1.0739
C	8	-0.9912	-2.0467	2.3886
C	9	-1.4265	-0.1665	-1.3642
C	10	-2.58	0.3452	-3.3369
C	11	-3.042	-1.0266	-2.8326
C	12	-0.9913	2.0438	-2.3953
C	13	-2.0555	-2.5524	-1.066
H	14	-2.9617	1.8085	3.6004
H	15	-4.0811	1.0098	2.4606
H	16	-3.4219	-1.0294	3.5492
H	17	-1.9519	-0.2762	4.234
H	18	-1.1337	2.5933	0.4748
H	19	-2.9233	2.7267	0.4246
H	20	-2.0072	3.3538	1.8279

H	21	-0.3081	-2.1576	1.5409
H	22	-0.3766	-1.9685	3.2999
H	23	-1.6467	-2.9266	2.4679
H	24	-3.4139	1.0232	-3.5641
H	25	-1.941	0.2616	-4.2339
H	26	-2.9625	-1.8143	-3.5952
H	27	-4.0818	-1.0073	-2.4609
H	28	-0.3143	2.1617	-1.5436
H	29	-0.3702	1.9585	-3.3014
H	30	-1.6466	2.9229	-2.4859
H	31	-1.1399	-2.5951	-0.4688
H	32	-2.9302	-2.7184	-0.4148
H	33	-2.02	-3.3535	-1.8184
N	34	-2.1069	1.2709	1.7317
N	35	-1.7791	-0.8423	2.2027
N	36	-1.7802	0.8411	-2.2057
N	37	-2.109	-1.2703	-1.7276

Table S9. NBO charges of **5**.

Natural Population						
Atom	No	Charge	Core	Valence	Rydberg	Total
Ni	1	0.53438	17.99326	9.43502	0.03734	27.46562
Cl	2	-0.56082	9.99987	7.5497	0.01126	17.56082
Cl	3	-0.56058	9.99987	7.54945	0.01126	17.56058
C	4	0.26833	1.99913	3.67071	0.06183	5.73167
C	5	-0.26192	1.99942	4.24812	0.01438	6.26192
C	6	-0.26093	1.99942	4.24681	0.0147	6.26093
C	7	-0.44235	1.9994	4.4292	0.01374	6.44235
C	8	-0.44635	1.9994	4.43349	0.01346	6.44635
C	9	0.26821	1.99913	3.67082	0.06184	5.73179
C	10	-0.26106	1.99942	4.24695	0.0147	6.26106
C	11	-0.26188	1.99942	4.24809	0.01438	6.26188
C	12	-0.44641	1.9994	4.43355	0.01347	6.44641
C	13	-0.44223	1.9994	4.42907	0.01376	6.44223

H	14	0.21597	0	0.78105	0.00298	0.78403
H	15	0.20001	0	0.79522	0.00477	0.79999
H	16	0.21169	0	0.78546	0.00285	0.78831
H	17	0.20763	0	0.78741	0.00496	0.79237
H	18	0.23531	0	0.76162	0.00306	0.76469
H	19	0.19672	0	0.79882	0.00447	0.80328
H	20	0.20934	0	0.78824	0.00243	0.79066
H	21	0.23751	0	0.7596	0.00289	0.76249
H	22	0.21396	0	0.78216	0.00389	0.78604
H	23	0.197	0	0.80041	0.0026	0.803
H	24	0.21184	0	0.78533	0.00284	0.78816
H	25	0.20769	0	0.78733	0.00499	0.79231
H	26	0.21593	0	0.7811	0.00297	0.78407
H	27	0.20003	0	0.79519	0.00478	0.79997
H	28	0.23694	0	0.76017	0.00288	0.76306
H	29	0.21398	0	0.78212	0.0039	0.78602
H	30	0.19731	0	0.8001	0.00259	0.80269
H	31	0.23527	0	0.76167	0.00306	0.76473
H	32	0.19675	0	0.79877	0.00449	0.80325
H	33	0.20933	0	0.78825	0.00242	0.79067
N	34	-0.33645	1.99933	5.31481	0.0223	7.33645
N	35	-0.35187	1.99935	5.33047	0.02205	7.35187
N	36	-0.35167	1.99935	5.33024	0.02208	7.35167
N	37	-0.33659	1.99933	5.31496	0.0223	7.33659
Total		0	65.98387	103.5615	0.45466	170

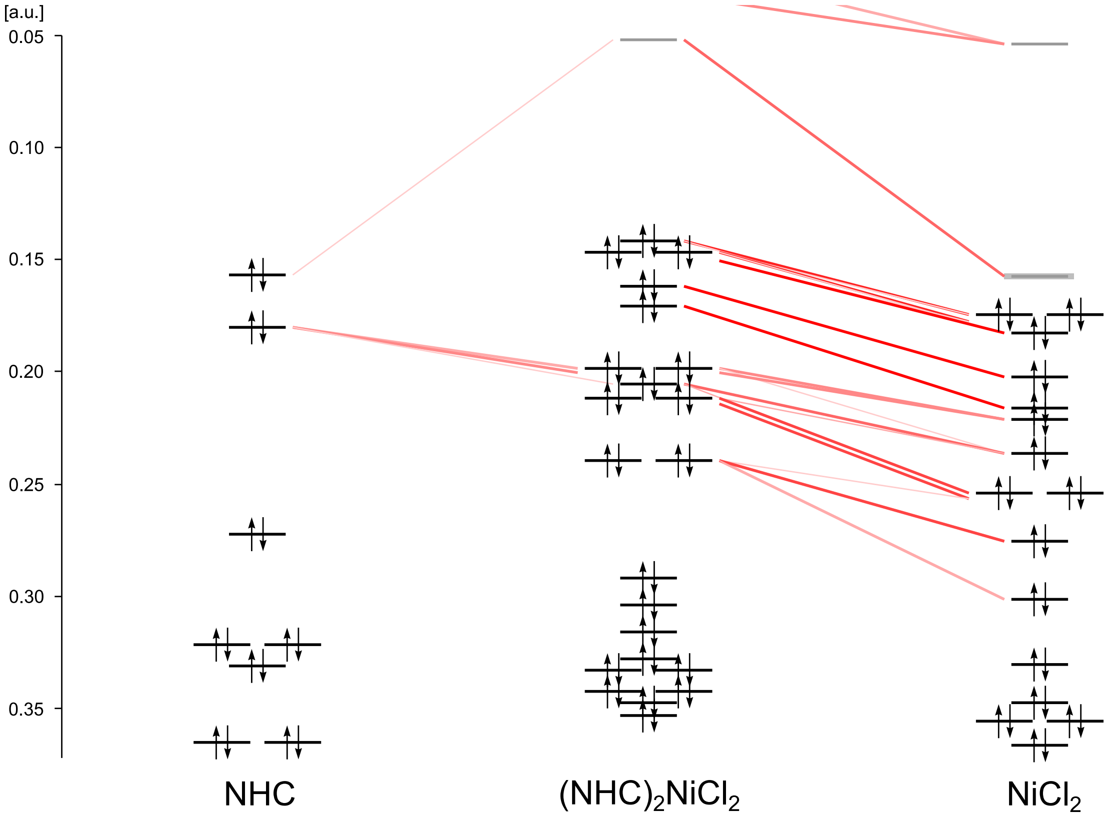

Figure S31. Correlation diagram of **3a**. Left column: NHC-fragment molecular orbitals; Middle column: full complex molecular orbitals; Right column: $NiCl_2$ molecular orbitals. The thickness of the lines corresponds to the contribution of the fragment molecular orbitals to the complex molecular orbitals.

5. Thermogravimetric Analysis

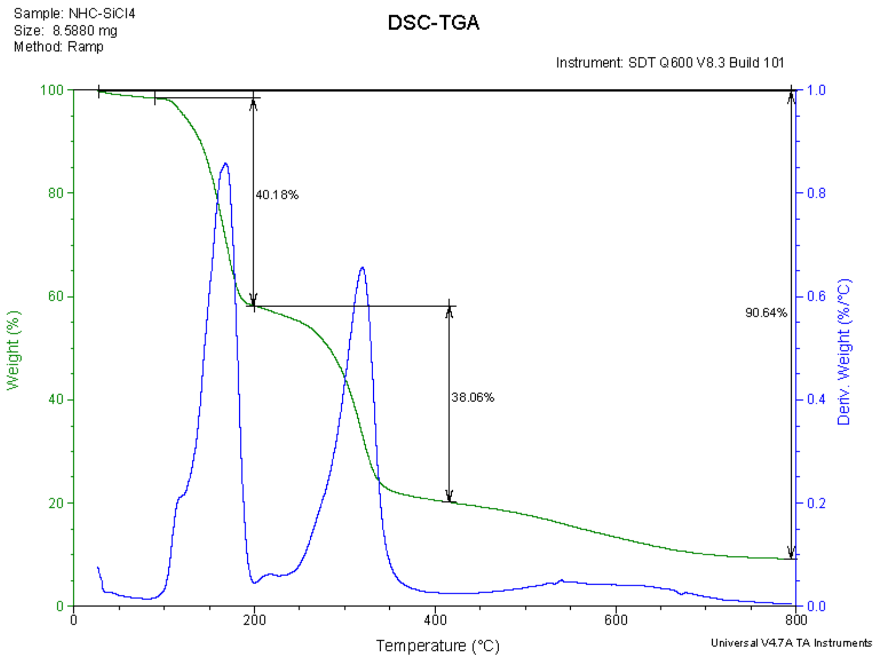

Figure S32: TGA diagram for **2**.

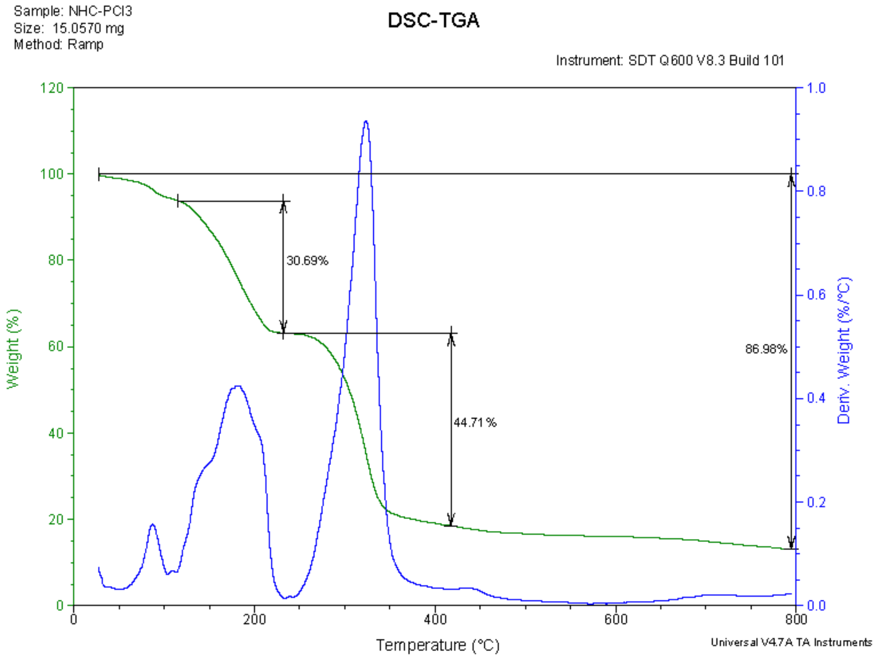

Figure S33: TGA diagram for **3a**.

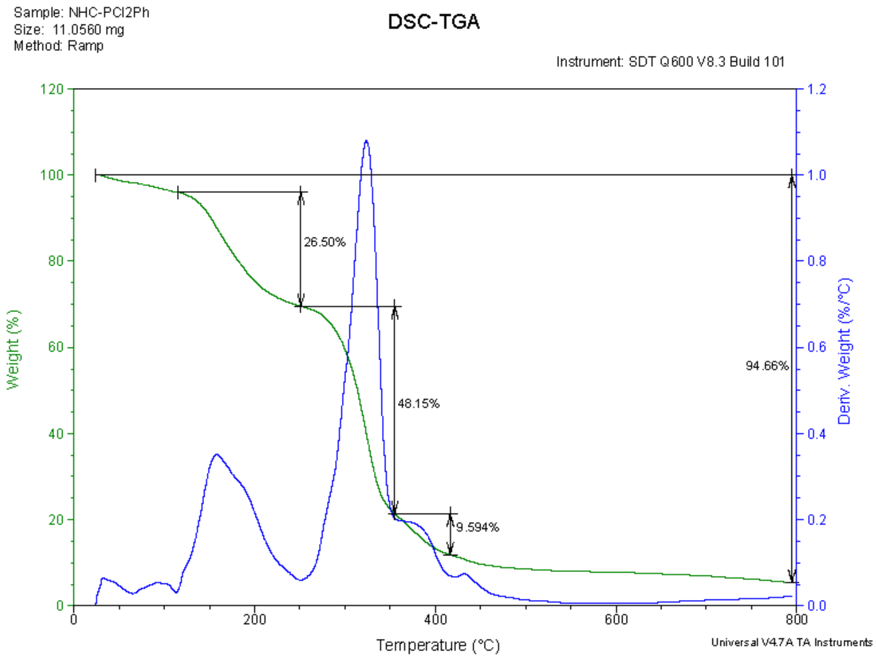

Figure S34: TGA diagram for **3b**.

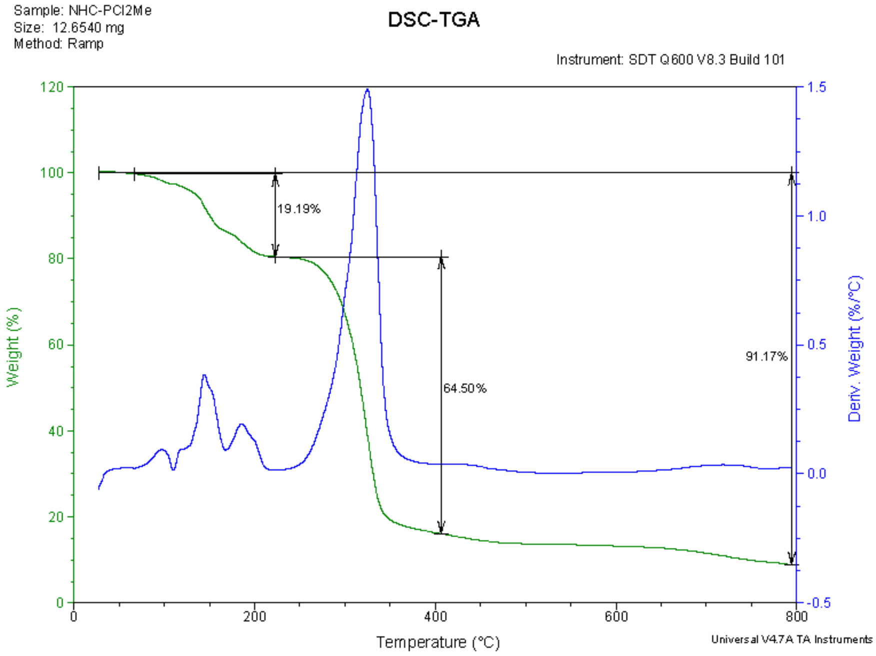

Figure S35: TGA diagram for **3c**.

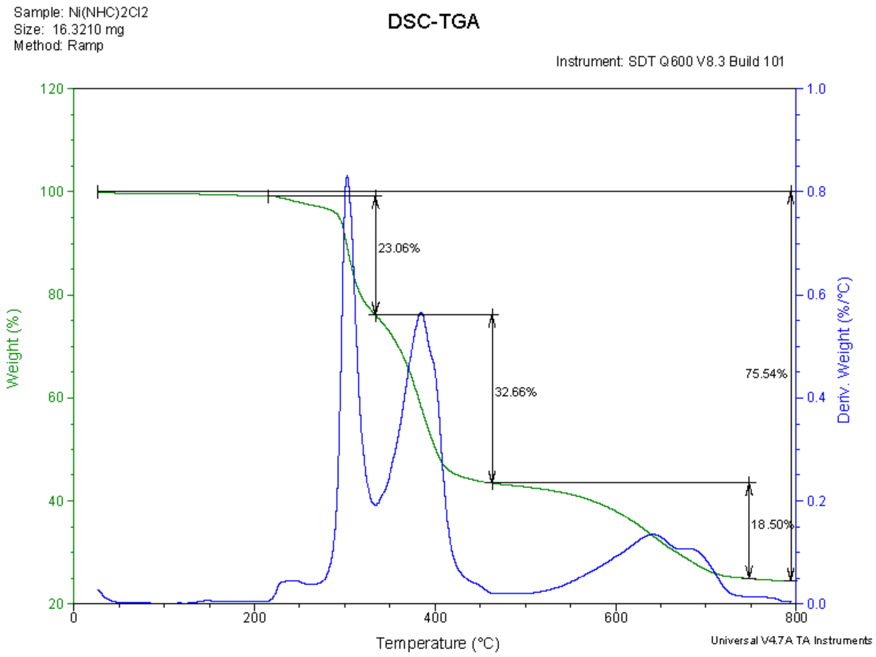

Figure S36. TGA diagram of **5**.

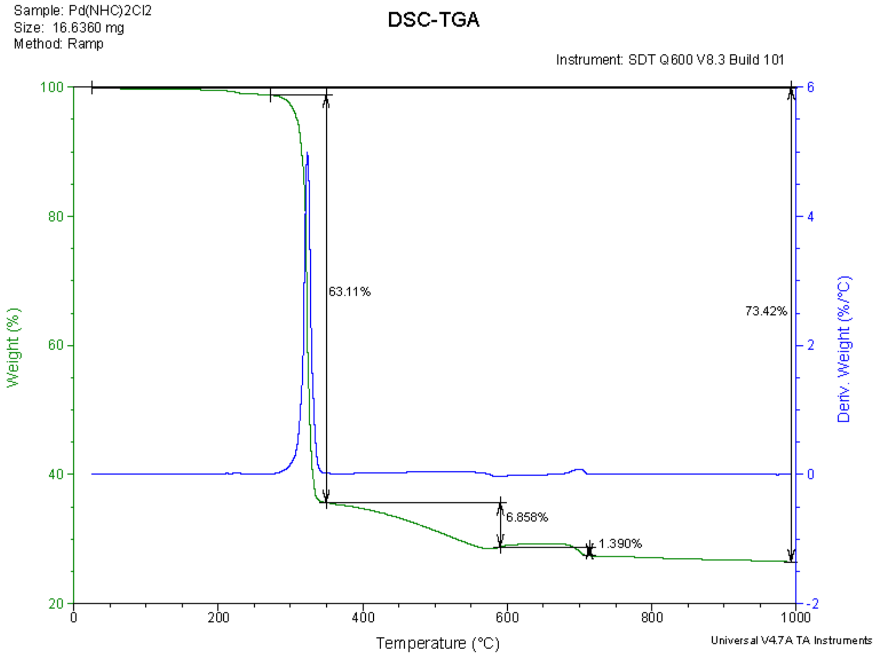

Figure S37: TGA diagram of **6**.

6. References

[1] G. M. Sheldrick, *Program for empirical X-ray absorption correction*; Bruker-Nonius, 1990.

[2] G. M. Sheldrick, *Acta Crystallogr., Sect. A: Found. Crystallogr.* 2008, **64**, 112.

[3] W. Kohn, L. J., Sham *Phys. Rev.* 1965, **140**, A1133.

[4] (a) G. te Velde, F. M. Bickelhaupt, E. J. Baerends, C. Fonseca Guerra, S. J. A. van Gisbergen, J. G. Snijders, T. Ziegler, *J. Comput. Chem.* 2001, **22**, 931.(b) C. Fonseca Guerra, J. G. Snijders, G. te Velde, E. J. Baerends, *Theor. Chem. Acc.* 1998, **99**, 391.

[5] J. P. Perdew, K. Burke, M. Ernzerhof, *Phys. Rev. Lett.* 1996, **77**, 3865.

[6] E. v. Lenthe, E. J. Baerends, J. G. Snijders, *J. Chem. Phys.* 1993, **99**, 4597.

[7] NBO 5.0. E. D. Glendening, J. K. Badenhoop, A. E. Reed, J. E. Carpenter, J. A. Bohmann, C. M. Morales, and F. Weinhold (Theoretical Chemistry Institute, University of Wisconsin, Madison, WI, 2001); http://www.chem.wisc.edu/~nbo5.

[8] R. F. W. Bader, *Chem. Rev.* 1991, **91**, 893.

[9] Z. Liu, *J. Phys. Chem. A*, 2009, **113**, 6410-6414.

[10] G. Frenking, W. Wichmann, N. Fröhlich, C. Loschen, M. Lein, J. Frunzke, V. M. Rayón *Coord. Chem. Rev.* 2003**, 238-239**, 55-82.